JOURNAL OF MATERIALS SCIENCE 32 (1997) 561–565

The effect of Si on the relationship between orientation and carbide morphology in high chromium white irons

G. POWELL
CSIRO Division of Manufacturing Technology, Adelaide Laboratory, PO Box 4, Woodville, SA 5011, Australia

V. RANDLE
Dept of Materials Engineering, University College of Swansea, Swansea, SA2 8PP, UK

Electron back-scatter diffraction (EBSD) has been shown to be the most appropriate technique to study the orientation and carbide morphology of small ($< 0.5\ \mu m$) regions of microstructure of high chromium white irons. The carbides in a slightly hypo-eutectic Fe–Cr–C alloy show a distinct texture close to $[1\,0\,\bar{1}\,1]$ whereas those in a 1.3 wt% Si commercial white iron have a diffuse texture, with regions near to major crystal directions, i.e., $[0\,0\,1\,1]$, $[\bar{1}\,2\,\bar{1}\,0]$, $[0\,1\,\bar{1}\,0]$, unpopulated. Using EBSD, it has been shown that the interconnectivity of the eutectic $(Cr, Fe)_7C_3$ carbide is less in a 1.3 wt% Si alloy compared with a low (0.1 wt%) Si alloy. This reduced interconnectivity is consistent with the increased fracture toughness in the as-cast condition.

1. Introduction

The microstructure of high chromium white irons in the as-cast condition consists of eutectic carbide, (M_7C_3) in a matrix of austenite and a small quantity of martensite and precipitated secondary carbides. It has been demonstrated that the morphology of the eutectic carbide phase is bundles of interconnected rods having a hexagonal cross-section [1]. This interconnectivity of the eutectic carbide is responsible for the low fracture toughness of the alloy. Discontinuities in the carbide rods can be produced by a high temperature ($\sim$ 1473 K) heat-treatment [2]. Such discontinuities increase the fracture toughness [3].

Some time ago, Diesburg and Borik [4] reported that increasing the silicon content in an 18% Cr–2% Mo–1% Cu–3% C (all compositions are given in wt%) iron from 0.4 to 1.2–1.6% substantially increased the k_{IC} fracture toughness, k_{IC}, in the as-cast condition. Diesburg and Borik were unable to offer an explanation for this unexpected increase in the fracture toughness as a result of an increased silicon content.

Electron back-scatter diffraction (EBSD) has been previously shown to be an immensely valuable tool in the crystallographic analysis of white irons [5, 6]. EBSD allows the orientation of regions of microstructure $< 0.5\ \mu m$ in size to be measured on an individual basis, from which information trends in the microtexture of individual phases can be collated. Strain in the microstructure can also be monitored qualitatively by observation of the diffraction pattern blurredness. A particular application of EBSD to white irons is that the microtexture of each phase can be monitored concurrently and related to the microstructure. These benefits are not available using X-ray texture techniques; neither is transmission electron microscopy the optimum tool for the examination of white irons since the "*in-situ* composite" nature of the material and the size of the carbides, typically a few microns in diameter, present difficulties. EBSD has been used in the presented work to measure individual areas of carbide in a polished section: where the orientations from such measurements are the same, it can be inferred that they have arisen from connected branches of the same carbide.

Previous work has shown that undercooled hypereutectic Fe–Cr–C alloy rapidly grown from the melt has a eutectic carbide morphology consisting of fine rods joined together and having a weak $[1\,0\,\bar{1}\,1]$ microtexture and no evidence of simple twinning [7]. When 1.6% Si is added to 18% Cr white irons, the nucleation of the eutectic M_7C_3 carbide is inhibited [8]. The present work aims to extend these preliminary results to correlate microstructure with morphology in these alloys and hence explain how a continuous connected carbide morphology has developed and whether the addition of 1.2–1.6% Si affects this development thus increasing the fracture toughness.

2. Experimental procedure

Orientations from two specimens were analysed using EBSD. They were:

(i) A ternary Fe–Cr–C (18% Cr, 2.8% C and 0.1% Si) hypoeutectic alloy cooled slowly at 45 °C per min from the melt to 1000 °C then water

0022–2461

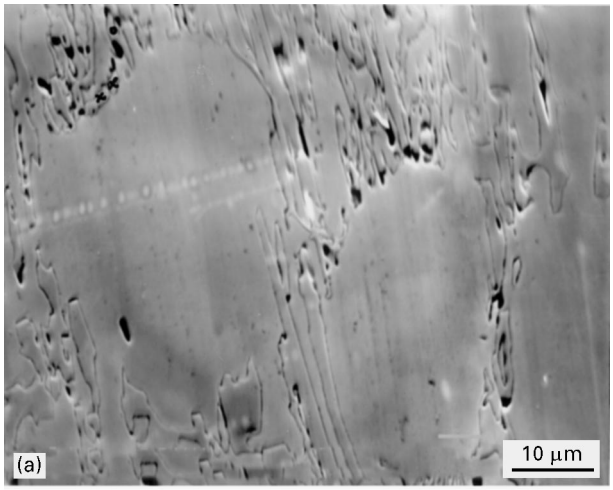

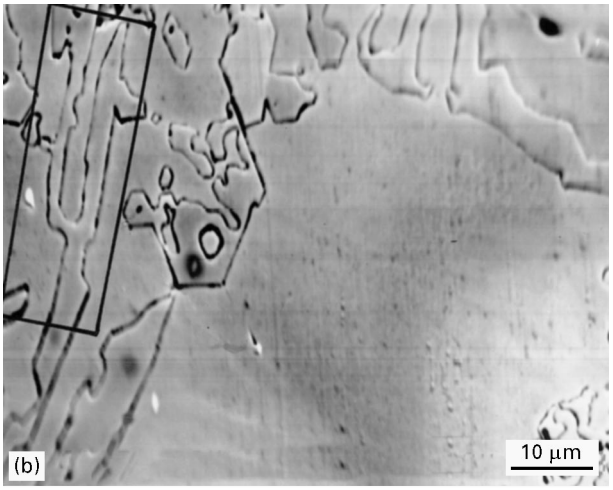

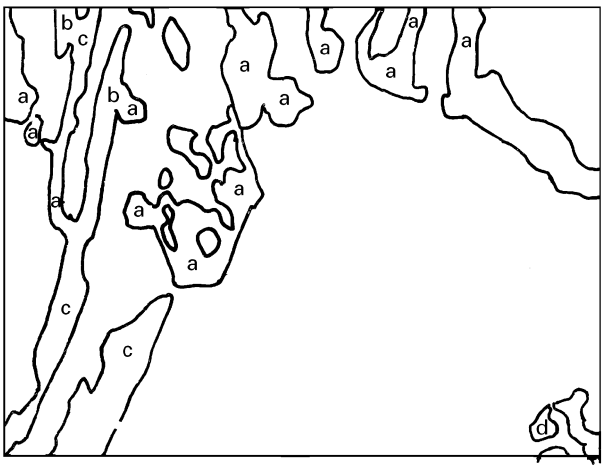

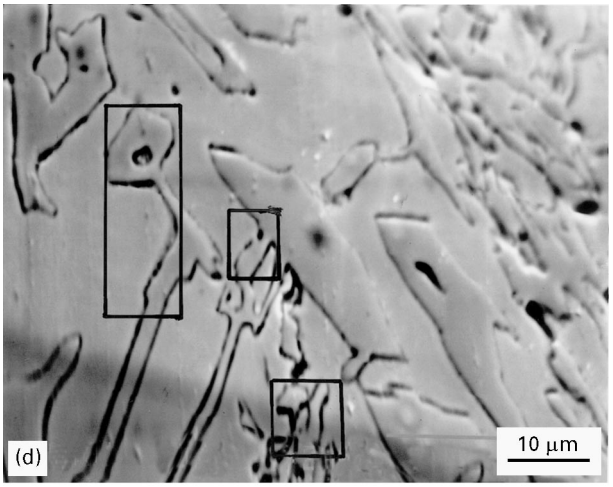

Figure 1 Microstructure of the Fe–Cr–C alloy. (a) Area showing sampling points in the matrix (contamination marks). All the carbides have a similar orientation except for those marked. (b), (d) examples of orientation-sampled areas with accompanying overlays ((c), (e) respectively) upon which similar orientations are indicated by the same letter. Areas in rectangular boxes contain dissimilar orientations.

quenched. The cooling has produced a microstructure of austenite dendrites with a coarse and fine eutectic of M_7C_3 plus austenite as is shown in Fig. 1(a–e).

(ii) A remelt of a high chromium commercial white iron, having 16% Cr, 1.5% Mo 1.69% Ni, 0.6% Cu, 3.0% C and 1.3% Si. The sample was cooled under similar conditions to the Fe–Cr–C alloy. The significant microstructural difference between the Fe–Cr–C alloy and the 1.3% Si commercial white iron is that for the latter eutectic solidification was complete before the water quench. The microstructure is shown in Fig. 2(a–e).

The specimens were prepared by a combination of polishing in colloidal silica and electropolishing in 5% perchloric acid at 40V, $-20\,^{\circ}C$, for about 20 s. The EBSD measurements were carried out using a diffraction system interfaced to a JEOL 6100 microscope. The principles and practice of EBSD are described in detail elsewhere [9].

Many of the regions selected for evaluation contained carbide colonies which were either nearly parallel or perpendicular to the plane of polish. Orientations were measured at several positions in individual carbide blades and rods, and also in the surrounding austenite matrix. Either the diffraction pattern was formally indexed on-line and saved to a data file, or the pattern was simply observed in real time while the probe was scanned across various regions of the microstructure, i.e., along carbide rods/blades and throughout the matrix, to monitor pattern changes.

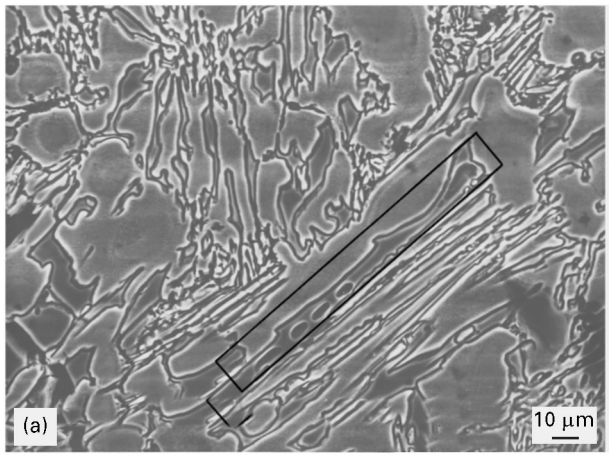

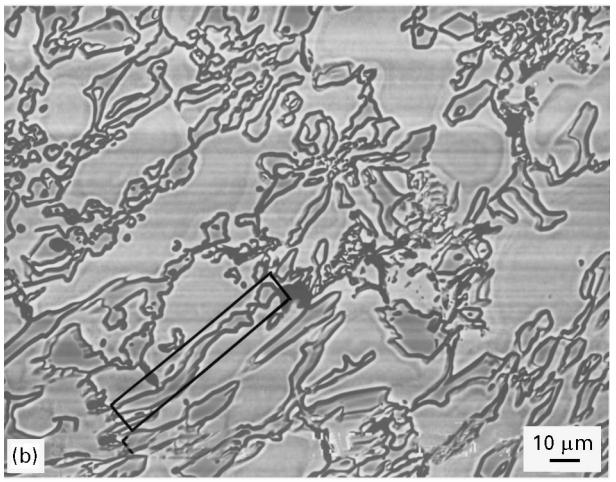

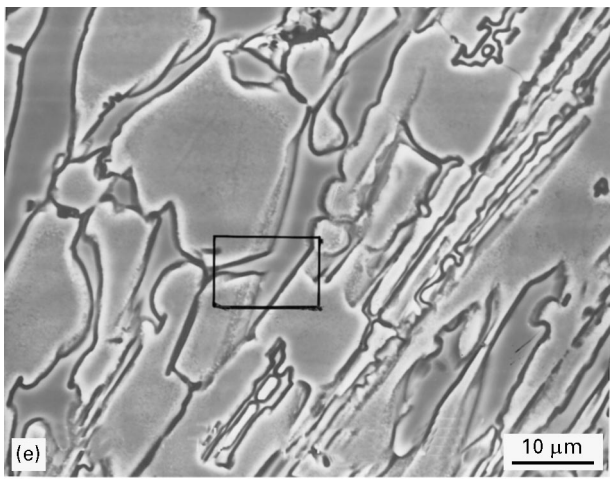

Figure 2 Microstructure of 1.3% Si commercial white iron. (a), (b) examples of orientation-sampled areas with accompanying overlays ((c), (d) respectively) upon which similar orientations are indicated by the same letter. Areas in rectangular boxes contain dissimilar orientations.

Where the pattern was observed to change, a quantitative orientation evaluation was made and stored.

3. Results

The "primary data" from the EBSD experiments consisted of an orientation, measured relative to fixed axes in the microscope, for specific points on each specimen in eight or more separate areas. Standard data output from the EBSD software is in the form of inverse pole figures (IPFs) or pole figures. Further data processing is required to extract more detailed information, i.e., comparison of three-dimensional orientation information from identified parts of the microstructure.

First, all the data obtained for both carbides and matrix in each specimen were considered overall. There was a noticeable difference between the quality (i.e., blurredness) of diffraction patterns taken from the matrix of the Fe–Cr–C alloy and the 1.3% Si commercial white iron; the former were far more blurred than the latter. This is demonstrated by comparison of the two diffraction patterns, arising from the austenite phase of the Fe–Cr–C alloy and the 1.3% Si commercial white iron, as shown in Fig. 3(a and b) respectively. Furthermore, in addition to the inferred strain in the Fe–Cr–C alloy there were pattern shifts of a few degrees over distances of approximately 1 μm. The scatter across one region of matrix in the Fe–Cr–C alloy was investigated; the misorientation between the fourteen sampling points is 2.6° on average, ranging from 0.6–4.3°. The row of sampling points is evident in

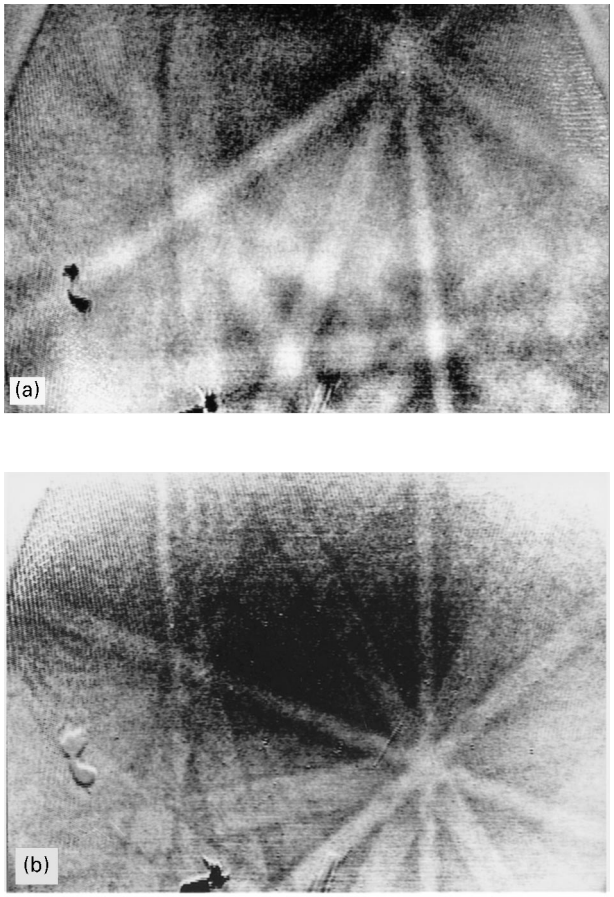

Figure 3 Electron back-scatter diffraction patterns from the matrix of (a) Fe–Cr–C alloy and (b) 1.3% Si commercial white iron showing evidence of more lattice strain in the former.

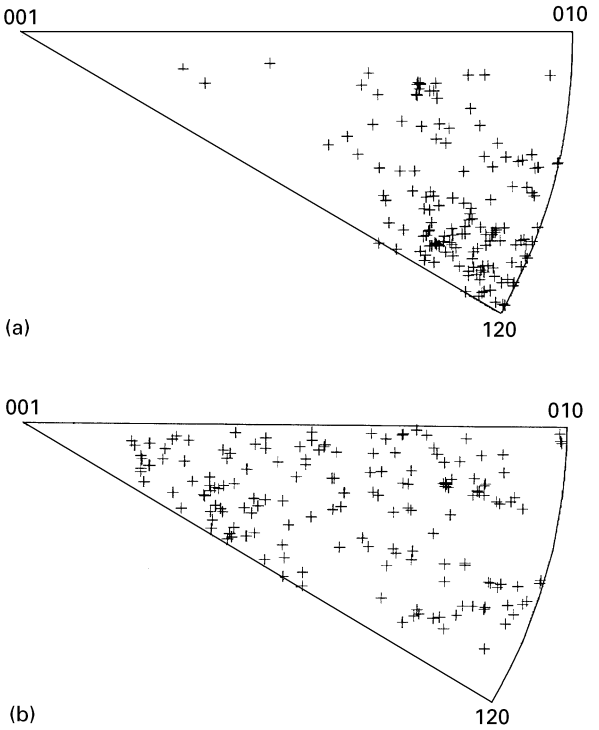

Figure 4 Inverse pole figures (normal direction) from (a) carbides in Fe–Cr–C alloy, (b) carbides in 1.3% Si commercial white iron. There is a far stronger microtexture in the Fe–Cr–C alloy.

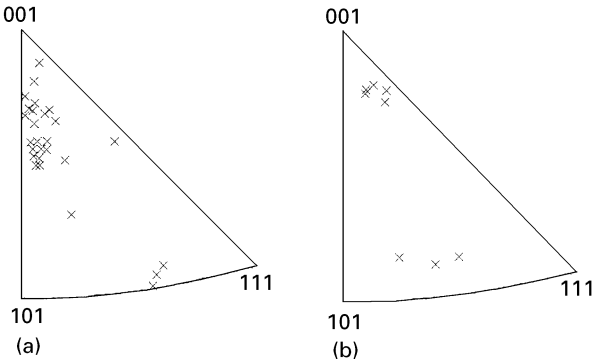

Figure 5 Inverse pole figures (normal direction) from (a) the matrix in Fe–Cr–C alloys, (b) matrix in 1.3% Si commercial white iron.

Fig. 1a. All these observations are evidence of considerable lattice strain in the Fe–Cr–C alloy which was absent in the 1.3% Si commercial white iron.

The overall microtexture of the two specimens was very different. Fig. 4(a and b) show IPFs (specimen surface normal direction) from carbides in the Fe–Cr–C alloy and the 1.3% Si commercial white iron. The former shows quite a distinct texture close to $[1\,0\,\bar{1}\,1]$ whereas the latter has a diffuse texture, with regions near to major crystal directions, i.e., $[0\,0\,1\,1]$, $[\bar{1}\,2\,\bar{1}\,0]$, $[0\,1\,\bar{1}\,0]$, unpopulated. In almost every sampled area a matrix orientation was also measured, and these are shown on IPFs in Fig. 5(a and b). A near $[1\,2\,0]$ direction normal to the specimen surface is apparent for the Fe–Cr–C alloy. The orientation relationship between a carbide having a normal direction very near $[0\,1\,\bar{1}\,0]$ and the adjacent matrix with orientation near $\{1\,0\,0\}\,\langle 0\,0\,1\rangle$, i.e., an "idealized case", is 27°/100, implying a simple orientation relationship between matrix and carbide for this specimen.

Individual orientation were output in numerical format as Euler angles. Figs. 1(a–e) and 2(a–e) include examples of the orientations mapped onto overlays of the micrographs in order to show the orientation at each quantitatively sampled location. The Euler angle tables were analysed carefully in order to identify and group like orientations, i.e., those for which the orientation difference was within 10° and so it was inferred that they represented *the same carbide grain.* Visual tracking of pattern changes which was noted during data collection was used to confirm the grouping process. The carbide grains are labelled a, b, c etc on Fig. 1(c and e) and Fig. 2(b and d). The letters represent the diffraction patterns actually indexed during the investigation, which does not include points where the diffraction pattern was inspected and found to be so similar to the previous pattern that it was not re-indexed. Also use of the same letters on different micrographs does not imply that the orientations are the same.

It is estimated that the orientation determinations are accurate to 3° for the cases reported here. This slightly degraded accuracy is because often the patterns were only of intermediate quality, due to the compromise in specimen preparation necessary to obtain patterns concurrently from the matrix and carbides. Sometimes the observed shifts between

diffraction patterns were up to 10° — this is a real effect since shifts of this magnitude were confirmed visually. These have been counted in the same group, i.e., as the same carbide.

Figs. 1(a–e) and 2(a–e) show the relationship between a few of the sampled orientations and the microstructure. The areas investigated included carbide rods parallel to the specimen surface, perpendicular to the surface, and intermediate rod geometries, as seen in Figs. 1(a–e) and 2(a–e). Orientation features of particular interest are those outlined by a rectangle in Fig. 1(b and d) and Fig. 2(a, b and e). If these are compared to regions on the respective overlays (Fig. 1(b and d) Fig. 2(c and d) it can be seen that they contain more than one orientation (within 10°) even though this is not indicated by any microstructural feature. In Fig. 1a, all the carbide orientations are the same except for those marked.

4. Discussion

The processing of the EBSD data reported above allows several deductions to be made about the carbide morphology, as follows. There were more local orientation changes in the 1.3% Si commercial white iron than in the Fe–Cr–C alloy, which is highlighted by the greater number of letters used on the orientation micrographs of the former. Where sections through adjacent carbides are coded by the same letter (≡ orientation), the implication is that they are branches of the same carbide. Clearly then there is more connectivity of the carbide network in the Fe–Cr–C alloy than the 1.3% Si commercial white iron.

This effect of silicon in 1.3% Si commercial white iron in reducing the connectivity of the eutectic carbide network is the probable cause of the improved fracture toughness of high chromium white irons containing 1.2–1.6% Si reported by Diesburg and Borik [4]. The production of discontinuities by heat-treatment [2] has increased fracture toughness [3]. This variation in the connectivity of the eutectic carbide is supported by the greater strain in the Fe–Cr–C alloy with more connectivity of the eutectic carbide network. One of the authors [10] has shown that, during cooling of a high chromium white iron, strain is introduced as the result of a difference in the coefficient of thermal expansion between the M_7C_3 eutectic carbide rods and the austenitic matrix. Less strain implies less connectivity for the 1.3% Si commercial white iron.

There are some examples on both specimens where there is an orientation change within a carbide, or at adjacent sections through carbides, as discussed in the previous section. The orientation changes within a single sectioned carbide provide evidence that they are polycrystalline, even though the boundaries are not visible on micrographs. The inference of these different orientations in adjacent carbide sections is not entirely conclusive; they are probably from unjoined carbides, but since polycrystalline carbides are proved to be present, it is possible that they may be branches of the same carbide. As shown in Figs. 1(a–e) and 2(a–e), sections through carbide blades usually have the same orientation and are therefore connected.

The reason for the effect of silicon is not entirely clear. It does not appear that the effect of silicon is simply to change orientation and carbide morphology via undercooling as a texture near $[0\,1\,\bar{1}\,0]$ has been reported previously in an undercooled Fe–Cr–C alloy [7]. It is more likely that silicon as an element has an effect on the growth of the M_7C_3 eutectic carbide.

5. Conclusions

(1) There are clear microtextural differences between the white iron specimens, having undergone different cooling regimes, which are linked to the morphology of the carbides. The carbides in the Fe–Cr–C alloy show a distinct texture close to $[0\,1\,\bar{1}\,0]$ whereas those in the 1.3% Si commercial white iron have a diffuse texture, with regions near to major crystal directions, i.e., $[0\,0\,1\,1]$, $[\bar{1}\,2\,\bar{1}\,0]$, $[0\,1\,\bar{1}\,0]$, unpopulated. Both inverse pole figures and orientation micrographs show that carbides are more connected in the Fe–Cr–C alloy than in 1.3% Si commercial white iron.

(2) Less connectivity in the 1.3% Si commercial white iron is the probable cause of the higher fracture toughness in the as-cast condition when 1.2–1.6% Si is added.

(3) The polycrystalline nature of some carbide networks was also revealed.

References

1. G. L. F. POWELL, *Metals Forum* **3** (1980) 37.
2. G. L. F. POWELL, in Proceedings of Conference on Metals in Mining, May 1981, Queensland, Australia, p. 58.
3. R. W. DURMAN and D. W. J. ELWELL, UK Patent 2167 438A, (1985).
4. D. E. DIESBURG and F. BORIK, in Proceedings of Symposium on Materials for the Mining Industry, July 1974, Vail, Colorado, USA, p. 15.
5. V. RANDLE and G. LAIRD II, *J. Mater. Sci.* **28** (1993) 4245.
6. V. RANDLE and G. L. F. POWELL, *J. Mater. Sci. Lett.* **12** (1993) 779.
7. G. L. F. POWELL, R. A. CARLSON and V. RANDLE, *J. Mater. Sci.* **29** (1994) 4889.
8. G. LAIRD II and G. L. F. POWELL, *Metall. Trans.* **24A** (1993) 981.
9. V. RANDLE, "Microtexture determination and its applications", (Institute of Materials, London 1992).
10. J. V. BEE, G. L. F. POWELL and B. BEDNARZ, *Scripta Metall. Mater.* **31** (1994) 1735.

Received 17 May
and accepted 2 July 1996